

Dynamical model of electroweak pion production in the resonance region

T. Sato^a, B. Szczerbinska^b, K. Kubodera^b and T. -S. H. Lee^c

^a Department of Physics, Osaka University, Toyonaka, Osaka 560-0043, Japan

^b Department of Physics and Astronomy, University of South Carolina, Columbia, SC 29208, USA

^c Physics Division, Argonne National Laboratory, Argonne, IL , USA.

In this report, we will briefly review the dynamical model of pion electroweak production reactions in the Δ resonance region and report on our study of neutrino-nucleus reactions based on this model.

1. Introduction

It is well recognized that the precise knowledge of neutrino-nucleus reactions is crucial in analyzing neutrino oscillation experiments [1]. For neutrino reactions around 1 GeV, quasi-elastic scattering and pion production processes are the main reaction mechanisms. The pion production takes place through both non-resonant and resonance processes, and in the latter the Δ_{33} resonance plays a central role for neutrinos in the 1 GeV region. Since experimental data on the neutrino-nucleon reactions in the resonance region are not as extensive as electron scattering data, a theoretical study of the weak pion production amplitude will be valuable for the study of neutrino-nucleus reactions [2,3,4,5,6,7].

In the recent years, extensive studies on the electron- and photon-induced meson production reactions in the GeV region are in progress to investigate the nucleon resonance properties [8]. The objective of the N^* study is to understand the non-perturbative dynamics of QCD by testing the resonance properties against the prediction of QCD-inspired models and/or lattice simulations. Two of the present authors with their collaborators have developed a dynamical model for describing photo- and electro-production of pions off the nucleon around the Δ resonance region [2,3]. It has been shown that including the pion cloud effect in theoretical analyses can resolve a long-standing puzzle that the $N\Delta$ magnetic dipole transition form factor G_M predicted

by the quark model is about 40% lower than the empirical value. Furthermore, the predicted $E2$ G_E and $C2$ G_C form factors show pronounced Q^2 dependence due to the pion cloud effects, which suggests the deformation effects in the $N\Delta$ transition. This model is further extended to investigate neutrino reactions, which involve the axial-vector responses of hadrons [4,5]. The $N\Delta$ axial vector form factor G_A is found to contain large meson cloud effects.

The dynamical model starts from the non-resonant meson-baryon interaction and the resonance interaction, and the unitary amplitudes are obtained from the scattering equation. Fairly consistent descriptions of all the available data in the Δ resonance region have been obtained from the dynamical model. The well tested dynamical model for the single-nucleon case will be a good starting point for investigating the reaction dynamics of neutrino-nucleus reactions.

In this paper we give a short review of our dynamical model for meson production reactions in the delta resonance region. Subsequently we show the results of our first application of this model to neutrino-nucleus reactions in the delta production region.

2. Dynamical model

We briefly describe our dynamical model of pion photoproduction. We start from the interaction Hamiltonian (H) for the N, Δ, π, ρ and ω fields. By assuming that only ‘few-body’ states

are active in the energy region we are interested in, we can simplify the intrinsic many-body problem. The effects due to many-body states are absorbed in effective interaction operators. In our work, the effective ‘few-body’ Hamiltonian H_{eff} is derived from H using the unitary transformation method [9]. The resulting effective Hamiltonian H_{eff} is defined in a subspace spanned by πN , Δ , γN states and has the following form:

$$H_{eff} = H_0 + \Gamma_{\pi N \leftrightarrow \Delta} + \Gamma_{\gamma N \leftrightarrow \Delta} + v_{\pi N} + v_{\gamma N}. \quad (1)$$

Here $v_{\pi N}$ and $v_{\gamma N}$ are non-resonant interactions, which consist of the u- and s-channel nucleon exchange and t-channel pion and vector meson exchange processes shown in Fig. 1(a). The excitation of Δ is described by $\Gamma_{\pi N \leftrightarrow \Delta}$ and $\Gamma_{\gamma N \leftrightarrow \Delta}$ shown in Fig. 1(b). An important feature of our approach is that the effective Hamiltonian is energy independent. Hence the unitarity of the resulting amplitude is automatically satisfied. Furthermore, the non-resonant interactions $v_{\pi N}$ and $v_{\gamma N}$ are derived from the same unitary transformation and hence πN and γN reactions can be described consistently.

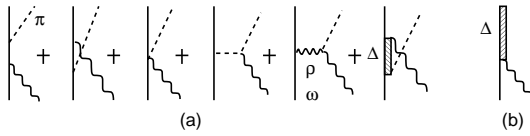


Figure 1. Graphical representation of $\gamma N \rightarrow \Delta$ and $\gamma N \rightarrow \pi N$ interactions.

From the effective Hamiltonian, it is straightforward to derive a set of coupled equations for πN and γN reactions. The resulting pion photoproduction amplitude is given as

$$\begin{aligned} T_{\gamma\pi} &= \langle \pi N | \epsilon \cdot J^{em} | N \rangle \\ &= t_{\gamma\pi}(W) + \frac{\bar{\Gamma}_{\Delta \rightarrow \pi N}(W) \bar{\Gamma}_{\gamma N \rightarrow \Delta}(W)}{W - m_\Delta^0 - \Sigma(W)}, \end{aligned} \quad (2)$$

where W is the invariant mass of the πN system. The first term is the non-resonant amplitude

$t_{\gamma\pi}$ calculated from the non-resonant interactions $v_{\pi N}$ and $v_{\gamma N}$. The second term in Eq. (2) is the resonant amplitude. The self-energy Σ is defined as

$$\Sigma(W) = \Gamma_{\pi N \rightarrow \Delta} G_0 \bar{\Gamma}_{\Delta \rightarrow \pi N}(W). \quad (3)$$

The ‘dressed’ $\gamma N \rightarrow \Delta$ vertex is defined by

$$\bar{\Gamma}_{\gamma N \rightarrow \Delta}(W) = \Gamma_{\gamma N \rightarrow \Delta} + \int \Gamma_{\pi N \rightarrow \Delta} G_0 t_{\gamma\pi}(W). \quad (4)$$

An important consequence of the dynamical model is that the influence of the non-resonant mechanisms on the resonance properties can be identified and calculated explicitly. The ‘bare’ resonance vertex $\Gamma_{\gamma N \rightarrow \Delta}$ is modified by the non-resonant meson cloud $t_{\gamma\pi}$ to give the dressed vertex $\bar{\Gamma}_{\gamma N \rightarrow \Delta}$.

3. Pion electroweak production and $N\Delta$ form factors

The dynamical approach described in the previous section was used to study π - N scattering, pion photoproduction and pion electroproduction reactions [2,3]. The model was subsequently extended to investigate neutrino induced reactions [4,5]. Since the weak currents in the standard model are closely related to the electromagnetic current, it is straightforward to extend the dynamical model of pion electroproduction to weak pion production reactions. The electromagnetic current (j_μ^{EM}), the weak charged current (j_μ^{CC}) and the weak neutral current (j_μ^{NC}) can be expressed in terms of the vector current V_μ and the axial-vector current A_μ as

$$j_\mu^{EM} = V_\mu^3 + V_\mu^{Iso-Scalar}, \quad (5)$$

$$j_\mu^{CC} = V_\mu^{1+i2} - A_\mu^{1+i2}, \quad (6)$$

$$j_\mu^{NC} = (1 - 2 \sin^2 \theta_W) j_\mu^{em} - V_\mu^{IS} - A_\mu^3. \quad (7)$$

Using CVC, $V_\mu^{1,2}$ can be obtained from V_μ^3 by isospin rotation. Guided by the effective chiral Lagrangian method and using the unitary transformation method, we can construct A_μ for pion production. The resulting A_μ consists of the nucleon-Born term, rho-exchange and delta excitation terms. The ‘bare’ $N\Delta$ magnetic and electric form factors $G_M(0)$ and $G_E(0)$ are obtained from the analysis of the (γ, π) reaction.

We assume the Siegert theorem to determine the Coulomb quadrupole form factor $G_C(0)$ from the transverse electric form factor $G_E(0)$. The Q^2 dependence of the form factors are assumed to be

$$G_\alpha(Q^2) = G_\alpha(0)R_{SL}(Q^2)G_D(Q^2), \quad (8)$$

where $G_D = 1/(1 + Q^2/m_V^2)^2$ is the dipole form factor of the proton with $m_V^2 = 0.71 \text{ GeV}^2$. The correction factor R_{SL} is defined as

$$R_{SL}(Q^2) = (1 + aQ^2) \exp(-bQ^2), \quad (9)$$

where $a = 0.154 \text{ GeV}^{-2}$ and $b = 0.166 \text{ GeV}^{-2}$ have been deduced by fitting the $(e, e'\pi)$ data at $Q^2 = 2.8$ and 4 GeV^2 [10]. For the $N\Delta$ axial vector form factor $G_A(Q^2)$, we also assume the form given in Eq. (8) with $G_D(Q^2)$ replaced by the nucleon axial-vector dipole form factor with $m_A = 1.02 \text{ GeV}$. We further assume the SU(6) quark model relation between G_A for the $N\Delta$ transition and g_A of the nucleon. Having determined the axial $N\Delta$ form factor, we have no further adjustable parameter in our model to describe neutrino-induced pion production reactions.

In Fig. 2, the energy dependences of the $p(e, e'\pi^+)n$ and $p(\nu, e^-\pi^+)p$ cross sections are shown at $Q^2 = 0.1(\text{GeV}/c)^2$ and $E_{lepton} = 1 \text{ GeV}$. The solid lines show the full results and the dashed lines show the contribution of the resonance amplitude which is the second term of Eq. 2. Clearly the non-resonant amplitude plays a crucial role. It is well known that the Kroll-Ruderman term dominates low-energy charged-pion production reactions. We note that even in the $p(\nu, e^-\pi^+)p$ reaction, where only the isospin 3/2 amplitude contributes, the non-resonant contribution to the cross section amounts to 15% at $W = 1.2 \text{ GeV}$. Thus the appropriate treatment of the non-resonant mechanisms plays an important role in interpreting the $N\Delta$ transition form factors $G_\alpha(Q^2)$ and also in determining the neutrino-nucleon reaction amplitudes that are needed for calculating the neutrino-nucleus reaction amplitudes.

The pion production mechanism of our dynamical model may be tested by comparing the theoretical and experimental values of the cross sections for a wide energy ranges also useful. For

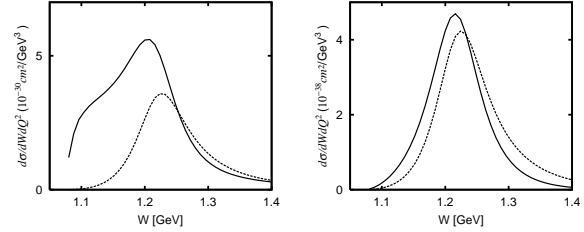


Figure 2. Cross section $d\sigma/dW/dQ^2$ of $p(e, e'\pi^+)n$ (left) and $p(\nu, e^-\pi^+)p$ (right) reactions.

instance, the longitudinal-transverse interference term $\sigma_{LT'}$ for a polarized electron is given by interference between the real and imaginary parts of the amplitude and hence it is sensitive to the non-resonant mechanism. As an example, we compare in Fig. 3 our predictions for the $e+p \rightarrow e'+p+\pi^0$ reaction with the Jlab data [11]. The cross section for virtual-photon pion production can be expressed as

$$\begin{aligned} \frac{d\sigma}{d\Omega_\pi} &= \left[\frac{d\sigma_T}{d\Omega_\pi} + \epsilon \frac{d\sigma_L}{d\Omega_\pi} \right] + \sqrt{2\epsilon(1+\epsilon)} \frac{d\sigma_{LT}}{d\Omega_\pi} \cos \phi_\pi \\ &\quad + \epsilon \frac{d\sigma_{TT}}{d\Omega_\pi} \cos 2\phi_\pi. \end{aligned} \quad (10)$$

The transverse cross section σ_T is mainly determined by the contribution of the magnetic dipole form factor G_M . Interference between the transverse and longitudinal currents (σ_{LT}) is sensitive to the product $G_C G_M$. Our model gives a reasonable description of the angular distribution from threshold to the delta resonance region. Reasonable agreement has also been seen in the comparison of our dynamical model predictions with the extensive pion production data in the delta resonance region obtained at LEGS, Mainz, Jlab and MIT-Bates.

We compare in Fig. 4 the calculated Q^2 dependence of the cross section for the $\nu_\mu + p \rightarrow \mu^- + \pi^+ + p$ reaction with the ANL [12] and BNL [13] data. Here we take into account the variation of the neutrino flux in the experiment and the finite mass of the muon. The results

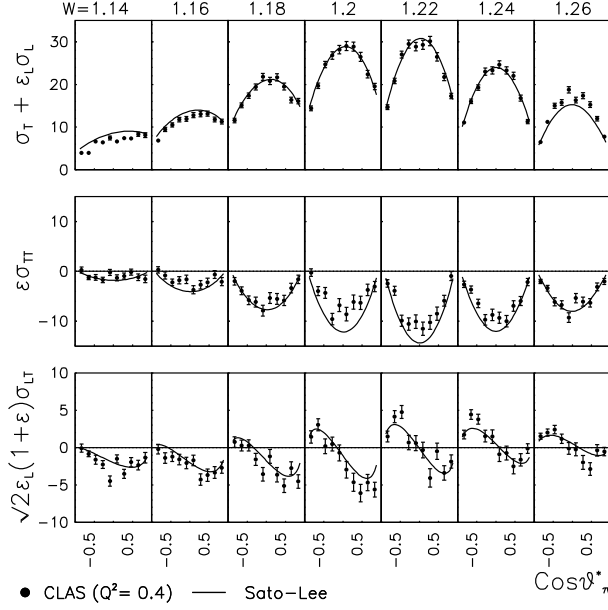


Figure 3. $p(e, e' \pi^0)p$ cross section at $Q^2 = 0.4(\text{GeV}/c)^2$.

of our full calculation (solid line) agree reasonably well with the data both in magnitude and Q^2 dependence. The contribution of the axial vector current (dashed curve) and the vector current (dot-dashed curve) have rather different Q^2 dependences in the low Q^2 region and interfere constructively with each other. Since the vector current contributions are highly constrained by the $(e, e' \pi)$ data, the results in Fig. 4 suggest that our model for the axial vector current reaction is consistent with the data. This in turn implies that the axial-vector $N\Delta$ coupling constant predicted by the SU(6) quark model is consistent with the existing data of neutrino-induced pion production reactions in the Δ resonance region. A precise measurement of parity-violating asymmetry of inclusive $p(\bar{\nu}, e')$ can be used to improve the determination of the axial $N\Delta$ form factor [5].

Finally, we explore the effects of the pion cloud on the $N\Delta$ transition form factors. Fig. 5 displays the dressed magnetic dipole form factor, G_M ,

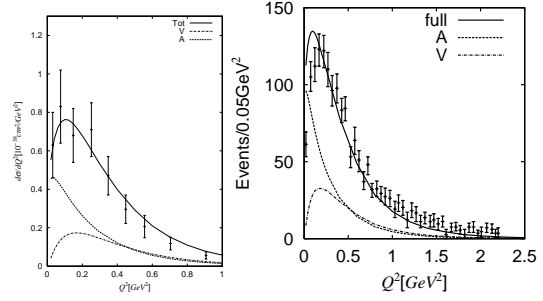


Figure 4. Differential cross section $d\sigma/dQ^2$ of $p + \nu_\mu \rightarrow \mu^- + \pi^+ + p$ reaction

and the dressed axial-vector form factor, G_A , extracted from our present model. The pion cloud effect is seen to be essential in explaining the empirical values of G_M directly extracted from the data. The pion cloud effects are sizable also for G_A . The dynamical model explains why most of the quark models underestimate G_M and G_A .

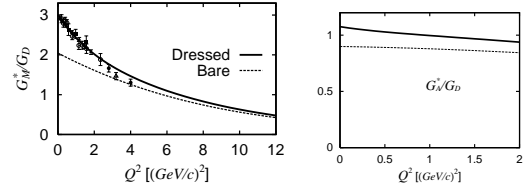


Figure 5. G_M (left) and G_A (right).

4. Neutrino-nucleus reaction

We now apply the dynamical model explained in the previous section to neutrino-nucleus reactions in the GeV region. The charged-current neutrino-nucleus reaction cross section can be

written as

$$\frac{d\sigma}{dE'd\Omega'} = \frac{p_l'}{p_l} \frac{G_F^2 \cos^2 \theta_c}{8\pi^2} L_{\mu\nu} W^{\mu\nu} \quad (11)$$

where $L^{\mu\nu}$ is the lepton tensor. The hadron tensor $W^{\mu\nu}$ is given as

$$W^{\mu\nu} = \sum_i \sum_f (2\pi)^3 \frac{E_T}{M_T} \delta^4(q + P_i - P_f) \langle f | J^\mu | i \rangle \langle f | J^\nu | i \rangle^*, \quad (12)$$

where $P_{i,f}$ is the initial or final hadron momentum, q a momentum transfer.

As a first step of our neutrino-nucleus reaction study, we consider the following points: (1) Fermi-averaging of the elementary amplitude is taken into account by calculating the reaction energy $W = \sqrt{(q + p_N)^2}$ of the elementary process from the nucleon momentum p_N inside nucleus and momentum transfer q . (2) We also take into account Pauli effects on the final nucleon after pion production. We require that the momentum of the final nucleon $|\vec{p}'| = |\vec{p}_N + \vec{q} - \vec{k}|$ be larger than the Fermi momentum. This correction is calculated for each pion momentum \vec{k} and initial nucleon momentum \vec{p}_N . Fig. 6 shows the cross section for the $\nu_e + {}^{12}\text{C} \rightarrow e^- + \pi + N + (A = 11)$ reaction divided by mass number for $E_\nu = 1$ GeV and for the two values of the lepton scattering angle, 10° and 30° . The dash-dotted curve shows the average of the cross sections for the proton and neutron targets, $(\sigma_p + \sigma_n)/2$. Fermi averaging is included in the dotted curve, and furthermore the Pauli-effect is included in the solid curve. As discussed in Ref. [6], the Pauli effect is appreciable at low momentum transfers, i.e. at forward lepton angles. In evaluating the Pauli effect, we take full account of the pion angular distribution as predicted by the dynamical model.

To examine to what extent our treatment can describe the data, we have studied inclusive electron scattering on ${}^{12}\text{C}$. The quasi-elastic process is evaluated using the relevant formula in Ref. [14]. The pion production process is calculated as described above. Here the nuclear correlation is taken into account by using the structure function given in Ref. [15]. In Fig. 7, our results are compared with the data for $E_e = 0.96$ and

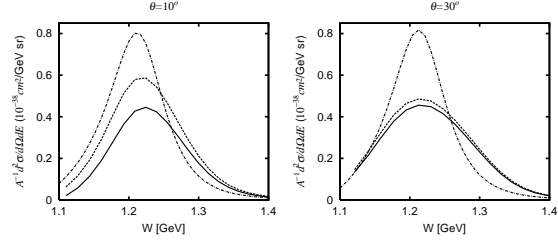


Figure 6. Cross section of $\nu + {}^{12}\text{C} \rightarrow e^- + \pi + X$.

1.1 GeV at $\theta = 37.5^\circ$ [16]. The magnitude of the calculated pion production cross section is comparable with the data, while our result (solid line) tends to overestimate the quasi-free cross section. Furthermore the ‘dip’ region between the quasi-free and delta-excitation peaks is not explained within the model.

Recently there have been detailed studies of nuclear effects in inclusive neutrino-nucleus reactions [17,18]. Meanwhile, in the present first attempt to apply the dynamical model of Refs. [2, 3,4,5] to neutrino-nucleus reactions, we have included nuclear-medium effects only by incorporating the Fermi-averaging and Pauli effects in the way described above and by introducing the structure function. It is obviously important to investigate any possible nuclear effects beyond the level considered in our present work.

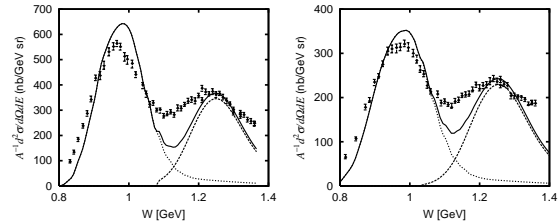


Figure 7. Inclusive cross section of ${}^{12}\text{C} + e \rightarrow e' + X$ at $E_e = 0.96$ GeV (left) and $E_e = 1.1$ GeV (right).

5. Summary

We have developed a dynamical model of electroweak pion production reactions. Most of the available data of pion electroproduction and neutrino reaction on the nucleon in the Δ region can be described reasonably well by the model. The $N\Delta$ transition form factors extracted from the data exhibit a large contribution of the pion cloud effects to the $N\Delta$ form factors, and these effects explain why the simple quark models fail to explain the magnitude and the Q^2 dependence of the empirical form factors. We have studied neutrino-nucleus reactions using the dynamical model that has been well tested by the electron scattering data. We have examined the effects of Fermi motion, Pauli blocking and nuclear correlations using the dynamical model. It is shown that these effects are important and significantly improve the description of the electron-nucleus scattering around 1 GeV. However further studies on the propagation of the Δ -particle in nuclei seem to be needed.

Acknowledgments

This work is supported by the Japan Society for the Promotion of Science, Grant-in-Aid for Scientific Research(c) 15540275, by the U.S. National Science Foundation, Grant Nos. PHY-0140214 and PHY-0457014, and by the U.S. Department of Energy, Nuclear Physics Division Contract No. W-31-109-ENG-38.

REFERENCES

1. J. G. Morfin and M. Sakuda and Y. Suzuki (eds), Proceedings of the First International Workshop on Neutrino-Nucleus Interactions in the Few GeV Region (NuInt01), Nucl. Phys. B(Proc. Suppl.) 112 (2002).
2. T. Sato and T.-S. H. Lee, Phys. Rev. C 54 (1996) 2660.
3. T. Sato and T.-S. H. Lee, Phys. Rev. C 63 (2001) 055201.
4. T. Sato, D. Uno and T.-S. H. Lee, Phys. Rev. C 67 (2003) 065201.
5. K. Matsui, T. Sato and T. -S. H. Lee, Phys. Rev. C 72 (2005) 025204.
6. E. A. Paschos, Ji-Young Yu and M. Sakuda, Phys. Rev. D 69 (2004) 014013.
7. O. Lalakulich and E. A. Paschos, Phys. Rev. D 71 (2005) 074003.
8. V. D. Burkert and T. -S. H. Lee, Int. J. Mod. Phys. E 13 (2004) 1035.
9. M. Kobayashi, T. Sato and H. Ohtsubo, Prog. Theor. Phys. 98 (1997) 927.
10. V. V. Frolov et al., Phys. Rev. Lett. 82 (1999) 45.
11. K. Joo et al., Phys. Rev. Lett. 88 (2002) 12001.
12. S. J. Barish et al., Phys. Rev. D 19 (1979) 2521.
13. T. Kitagaki et al., Phys. Rev. D 42 (1990) 1331.
14. R. A. Smith and E. J. Moniz, Nucl. Phys. B 43 (1972) 605.
15. O. Benhar, A. Fabrocini, S. Fantoni and I. Sick, Nucl. Phys. A 579 (1994) 493.
16. R. M. Sealock et al., Phys. Rev. Lett. 62 (1989) 1350.
17. O. Benhar et al., Phys. Rev. D 72 (2005) 053005.
18. J. Nieves et al., nucl-th/0503023.